BEHAVIOURS OF POLYMER-MODIFIED ASPHALT REINFORCED WITH GEOSYNTHETICS-A PHYSICAL MODEL STUDY

T. Chantachot[1], W. Kongkitkul[2], S. Youwai[3] , and P. Jongpradist [4]
[1] Graduate Student, Department of Civil Engineering,
King Mongkut's University of Technology Thonburi, Bangkok, Thailand,
[2, 3 & 4]Assistant Professor, ditto, Email: warat.kon@kmutt.ac.th

ABSTRACT

Many flexible pavements constructed of normal hot-mix asphalt (HMA) are susceptible to functional failures before their design life mostly by the excessive traffic loads. It seems that there are, at least, two countermeasures dealing with the construction materials for mitigating this problem. The former is to reinforce the HMA pavement by polymer geosynthetic reinforcement. The latter is to improve the pavement material by using polymer-modified asphalt (PMA). A number of experimental studies have been individually performed looking for effects of reinforcement on reduction of pavement settlement alone and for performances improved by using PMA alone. However, little is known on the behaviours of PMA pavement reinforced with polymer reinforcement. In this study, a series of laboratory physical model tests were performed on PMA pavements either unreinforced or reinforced with different types of polymer geosynthetic reinforcements. Then, vertical stress was cyclically applied on the pavement surface by means of a footing. It was found that: i) the residual settlement of the footing significantly decreased with PMA pavement reinforced with geosynthetic reinforcements; ii) the maximum shear strain in the soil layer supporting the pavement was significantly less developed and less localised with reinforced PMA pavement than the unreinforced pavement; and iii) using a geosynthetic reinforcement that had more contact area with pavement bottom resulted in much better performance.

Keywords: Geosynthetic reinforcement, pavement, polymer-modified asphalt, physical model test, strain field

INTRODUCTION

Flexible pavements, serving as paths for road transportations in many countries, are typically constructed from normal hot-mix asphalt (HMA). Due to the increasing of traffic factors such as traffic load, traffic volume, and tyre pressure, this HMA pavement is presently often damaged before its design life. And, this damage may results not only in the malfunctions of the pavement but also the danger to the road users. Considering all the above, it seems that it is necessary to improve the performance of the pavements constructed by the normal HMA.

A high performance pavement requires asphalt cement that is less susceptible to high temperature rutting and fatigue cracking. This led to a modification of normal asphalt cement to obtain the so-called "polymer modified asphalt cement (PM-AC)". The most commonly used polymer for this modification is styrene butadiene styrene (SBS) among others such as styrene butadiene rubber (SBR) and ethylene vinyl acetate (EVA) (Airey 2004). From a laboratory study by Sengoz and Isikyakar (2007), they found that SBS modification increased the softening point, reduced the penetration and increased the stiffness (hardness) of the Polymer Modified Bitumens (PMBs). PMBs may become less sensitive to residual deformation and rut depth decreased with increasing polymer percentages. Therefore, polymer modification typically improves fatigue and rutting resistances (Glover et al. 2005).

On the other hand, geosynthetic reinforcements, planar products manufactured from polymeric materials, have been introduced to reinforce the soil. The geosynthetics for reinforcing function include geogrid, geotextile and geocomposite (Koerner 2005). And, these geosynthetics have also been used to reinforce the pavement as well as its foundation soils in the road constructions. From a field study by Kulkarni et al. (1998), it was found that the reinforcing of pavement with geogrid increased the strength and therefore service life while decreased the vertical cracking. In addition, from a laboratory physical model study performed by applying not only monotonic load but also cyclic load on the new geogrid-reinforced flexible pavement by Ling and Liu (2001), they also found that the reinforcing of pavement was able to increase both the stiffness of relation between load and deformation and the strength. Furthermore, series of scaled-down physical model tests on new and overlayed pavement structures either unreinforced or reinforced with geosynthetic

reinforcements (e.g., Thaisri 2009; Kunakulsawat et al. 2010; Youwai et al. 2010) revealed that, when

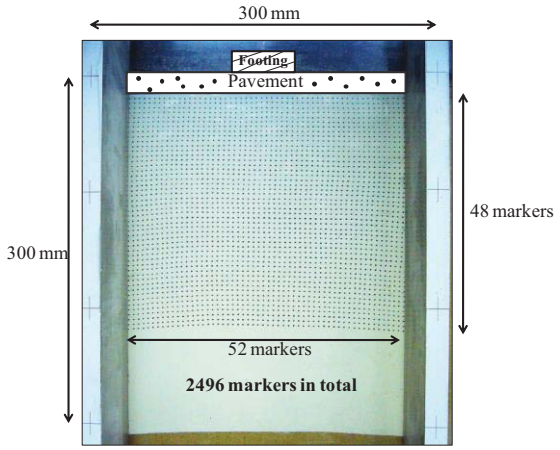

Fig. 1 Latex rubber sheet attached on the acrylic plate for observations of sand deformation during the test

reinforced with geosynthetic reinforcements: i) the residual deformation of pavement layer decreased; and ii) the distribution of maximum shear strains of base layer was uniform with its average value lower than when unreinforced.

Summarising the above, there are two methods for improving the performance of pavements constructed of normal HMA: i) replacing normal asphalt cement with the PM-AC having the same viscosity grade; and ii) reinforcing pavement with geosynthetic reinforcement. However, behaviours of combining together these two methods described above have been limitedly found in the literature. In this study, behaviours of geosynthetic-reinforced polymer modified asphalt (PMA) were therefore studied by performing a series of physical model test in the laboratory.

TEST MATERIALS, APPARATUSES AND METHODS

Test Materials

In the present study, cleaned uniform sand called "KMUTT sand" was used to model both the base and the subbase of the pavement structure model. This sand had D_{50} and C_u equal to 0.285 mm and 1.879, respectively. It was pluviated into the container (explained later) by a multiple sieving pluviation apparatus which was modified and constructed based on the typical pluviation pattern in preparation of sand specimen for triaxial test (i.e., Miura and Toki 1982). As a result, the pluviated sand inside the container was uniform and had a unit weight of 15 kN/m^3. In addition, the CBR value of sand prepared as above was 13.4 %.

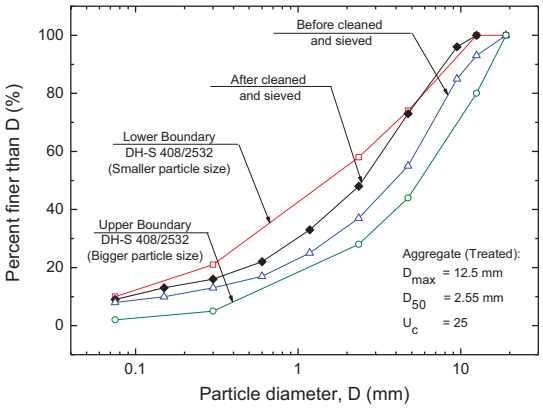

Fig. 2 Grain size distributions of aggregate used in this study

Prior to sand pluviation, 0.3-mm thick latex rubber sheets were attached on the inner surfaces of the acrylic plates (Fig. 1). To do so, a thin layer of silicone grease was smeared on to the acrylic surfaces and the latex rubber sheets were then attached on. This technique was used not only to reduce the friction between the sand and the acrylic plates but also to observe the sand deformations by photogrammetric analysis. It can be done by photographing of the markers printed on the latex rubber sheet in the square pattern (52x48=2496 markers). The photos of latex rubber sheet were taken by using a 5 Mega pixel digital camera. Then, the Cartesian coordinates (x, y) of each markers were digitised by a software. A source code in MATLAB computer program for calculation of strain for each elements can be created by based on the four-node isoparametric formulation. Subsequent, the strain contours were plotted by using Surfer program (Kongkitkul 2004).

Modelled PMA pavements were prepared by hot-mix procedures in the laboratory. A PM-AC having a penetration grade of 60/70 was used. This PM-AC was manufactured by following the standard number DH-SP 408/2536 of the Department of , Thailand (1993). The aggregate for mixing with PM-AC was prepared based on the standard number DH-S 408/2532 of the Department of Highways, Thailand (1989). Before use, it was sieved and washed with tap water. The grain size distribution curve of this aggregate is shown in Fig. 2. Then, after had been heated to 180 °C, the aggregate was mixed with PM-AC at the asphalt cement content of 5 %. This value was derived from a series of Marshal's test results (Thaisri 2009). Then, the mixture was compacted into a mould to prepare a 60 mm thick modelled

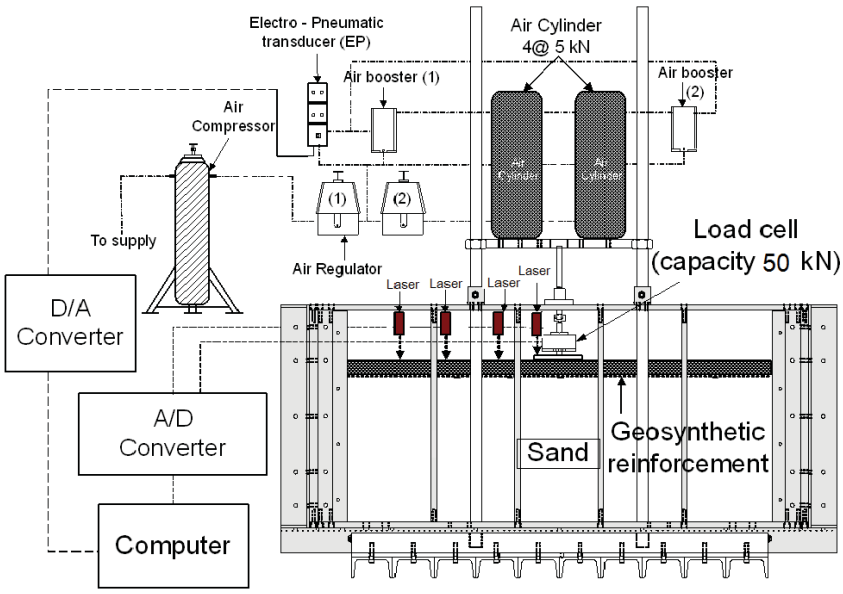

Fig. 3 Experimental set up of the scaled-down physical model of PMA pavement structures either unreinforced or reinforced with geosynthetic reinforcements

PMA pavement. Its density was controlled at 2.1 g/cm^3.It was then cured in mould for at least 16 hours before use.

Table 1 Physical properties of geosynthetic reinforcements used in this study

Properties	Geogrid	Geocomposite
Polymer type	Polyester	Polypropylene
Tensile strength (kN/m)		
Machine direction	50	50
Cross-machine direction	50	50
Aperture size (cm)	2	3
Machine direction	2	3
Cross-machine direction		
Mass per unit area (g/m^2)	335	300

Two types of geosynthetic reinforcements were used: i) geogrid; and ii) geocomposite. These are a biaxial polyester geogrid and a biaxial polypropylene continuous filament nonwoven geotextile reinforced by a network of glass filaments, respectively. The physical properties of the two types of geosynthetic reinforcements are listed in Table 1. Their installation position was at the bottom surface of the modelled PMA pavement. This was achieved by placing them at the mould bottom and adhering with tack coat before placing of the hot-mix PMA for compaction.

Container and Loading Apparatus

A container was used to prepare the scaled-down model of pavement structures in this study. It was 180 cm in width, 80 cm in height and 40 cm in depth (the out-of-plane direction). It consisted of acrylic plates at the front and rear sides, reinforced with metal frame and assembled with the steel plates at the end sides.

Figure 3 shows the experimental setup in this study. A modelled strip footing was used to vertically load on the centre of modelled PMA pavement placed on the pluviated sand surface. Its dimensions were 6 cm in width and 39.5 cm in length. Axial forces from four air cylinders were combined by a steel plate and the combined force was axially vertically transferred to the footing. A long linear bush was used for load vertical alignment. The axial load applied to the modelled footing was measured by an axial load cell while the footing settlement and surface settlements along the lengthwise of the modelled PMA pavement by four laser displacement sensors pointed at the footing centre and at the distances of 60, 150 and 300 mm from the footing centre.

Test Configurations

In this study, four test configurations were studied: 1) unreinforced PMA pavement; 2) geogrid-reinforced PMA pavement; 3) geocomposite-reinforced PMA pavement; and 4) PMA reinforced with both geogrid and geocomposite. Table 2 lists

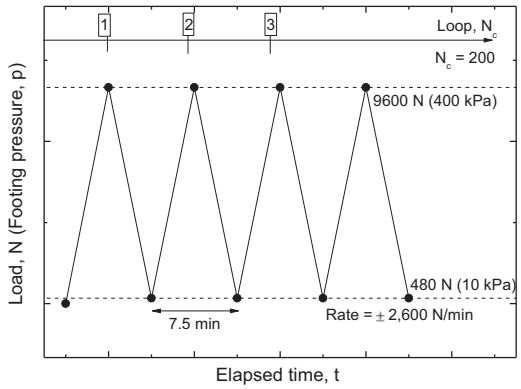

Fig. 4 Cyclic loading pattern applied to the modelled footing to load on the modelled PMA pavement in this study

Table 2 Test configurations in this study

No.	Names	Configurations
1	NPNO	Unreinforced
2	NPGG	Reinforced with geogrid
3	NPGT	Reinforced with geocomposite
4	NPGGGT	Reinforced with geogrid and geocomposite

the respective test names of these four configurations.

After having finished arranging the modelled footing and all the measuring devices, a series of cyclic loadings (CL) were applied to the footing and therefore to the pavement at a rate of ± 2,600 N/min (Fig. 4). The amount of footing pressure mobilised by these cyclic loadings (400 kPa; Figure 4) was determined based on one equivalent standard axial load of 18 kips (i.e., 50 kN) (AASHTO, 1993) acting on one wheel and then scaled-down to 40 % to be consistent with other materials modelled in this study. All the tests were performed in a laboratory under the controlled temperature of 25 ^{o}C

TEST RESULTS AND DISCUSSIONS

Footing Settlement

In this study, the residual deformation at the respective number of cycle (N_c) was defined as shown in Fig. 4. That is, at the beginning of the test, a constant-rate-of-load loading was applied until 400 kPa, and, at this moment, N_c was counted as one. Then, unloading was immediately performed until 10 kPa after which reloading was immediately applied immediately until 400 kPa, and, at this moment, N_c = 2 was counted. This process was continued until N_c = 200.

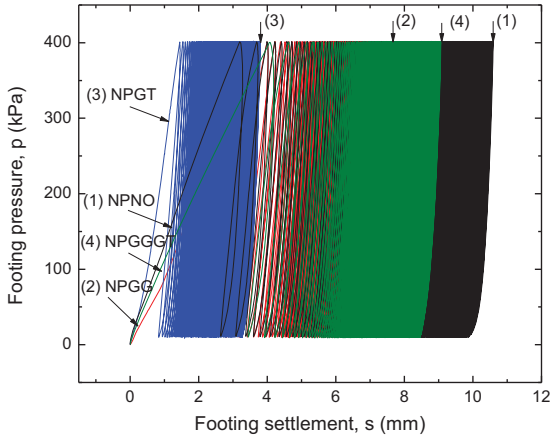

Fig. 5 Relationships between footing pressure (p) and footing settlement (s) for all the tests performed in this study

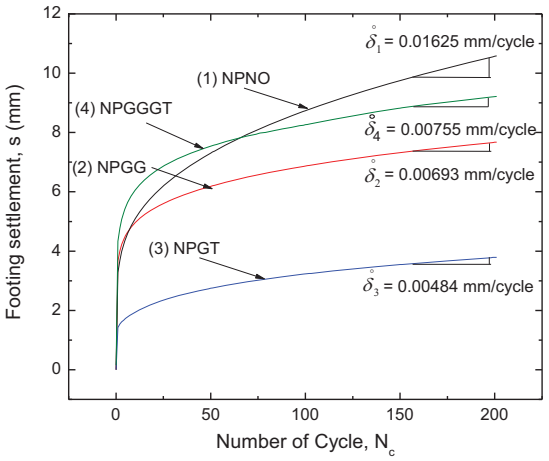

Fig. 6 Relationships between footing settlement (s) and number of cycle (N_c)) for all the tests performed in this study

Figure 5 shows the footing pressure (p) – footing settlement (s) relations for all the test configurations performed in this study. Figure 6 shows the respective subsequent s – N_c relations. It may be seen from these figures that the s mostly developed when N_c was less than 50 and the increment of s became smaller when N_c increased. This may due to that the pavement and, in particular, the sand underneath deformed plastically in some limited extents which also expanded during these first 50 cycles of CL. Then, when N_c became more than 50, it seemed that the zones where the plastic deformation formed became limited while the further developed s were due to the additional plastic deformation localised in the same zone. This will be explained in detail later from the results of photogrammetric analysis.

The footing settlements significantly decreased by reinforcing with geosynthetic reinforcements. That is, the unreinforced PMA pavement (NPNO)

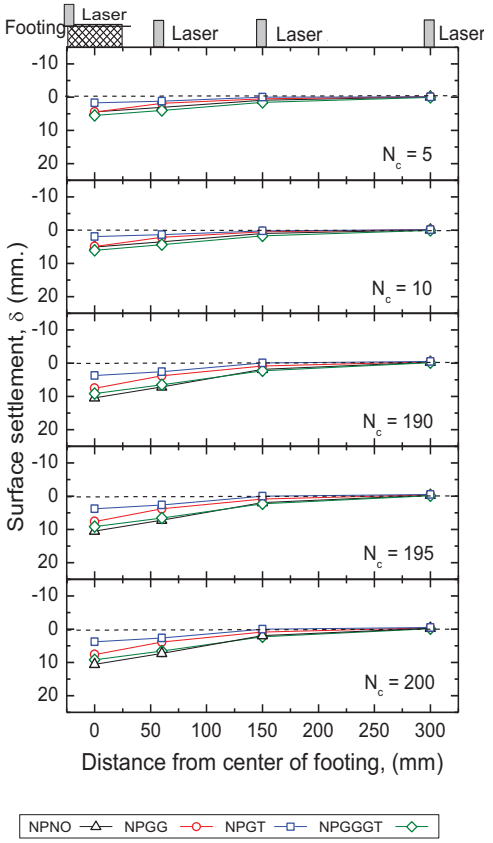

Fig. 7 Relationships between surface settlement and distance from the centre of footing for all the tests performed in this study

showed greater footing settlement than others. Then, the PMA pavement reinforced with both geogrid and geocomposite (NPGGGT), the one reinforced with geogrid (NPGG) and the one reinforced with geocomposite (NPGT) exhibited footing settlements from the second greatest to the smallest, respectively. It seemed that reinforcing pavement with geosynthetic reinforcement could distribute the footing pressure to the materials underneath in a much greater extent by that the overall rigidity of pavement was increased by the reinforcing effects.

Figure 6 also shows the rates of footing settlement development ($\dot{s}$) measured during the last several loops of CL before the ends of test. The $\dot{s}$ values were also decreased by reinforcing effects. That is, $\dot{s}$ for the NPGT equal to 0.00484 mm/cycle was the smallest among all the tests. The values for NPGG, NPGGGT and NPNO respectively equal to 0.00693, 0.00755 and 0.01625 mm/cycle were subsequently greater.

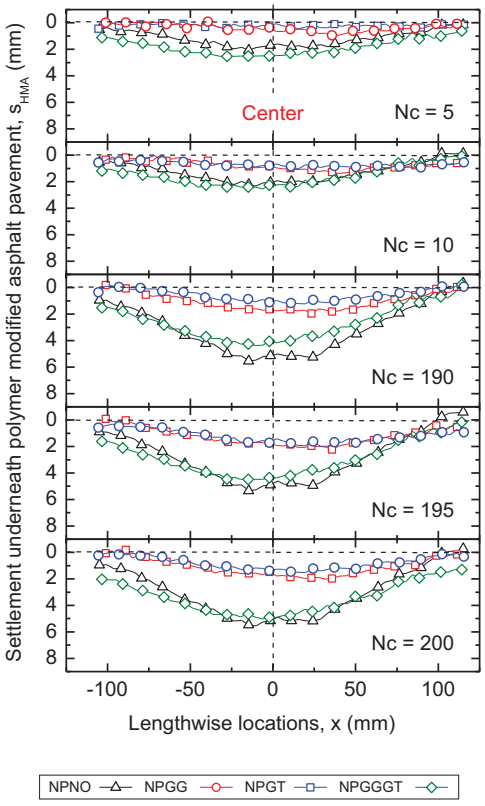

Fig. 8 Settlement underneath pavements determined from photogrammetric analyses for all the tests performed in this study

Surface Settlement and Settlement Underneath Pavement

The surface settlements along the pavements were measured by the four laser displacement sensors as shown in Fig. 7. According to Fig. 7, the surface settlements decreased with an increase in the distance from centre of footing. The values measured at 300 mm from the centre were nearly the same for different test configurations and also nearly zero. This fact confirmed that the length of pavements used in this study was sufficient for the size of footing used (i.e., 6 cm). When compared among different tests for the surface settlements at 60 and 150 mm from the centre other than the values at the centre which already compared in Figure 6, the values for NPNO, NPGGGT, NPGG and NPGGGT were respectively the greatest to the smallest, in the same order as for the footing settlements shown in Figure 6. This fact also confirms the effects of reinforcing with geosynthetic reinforcements on the developed overall rigidity of the pavement.

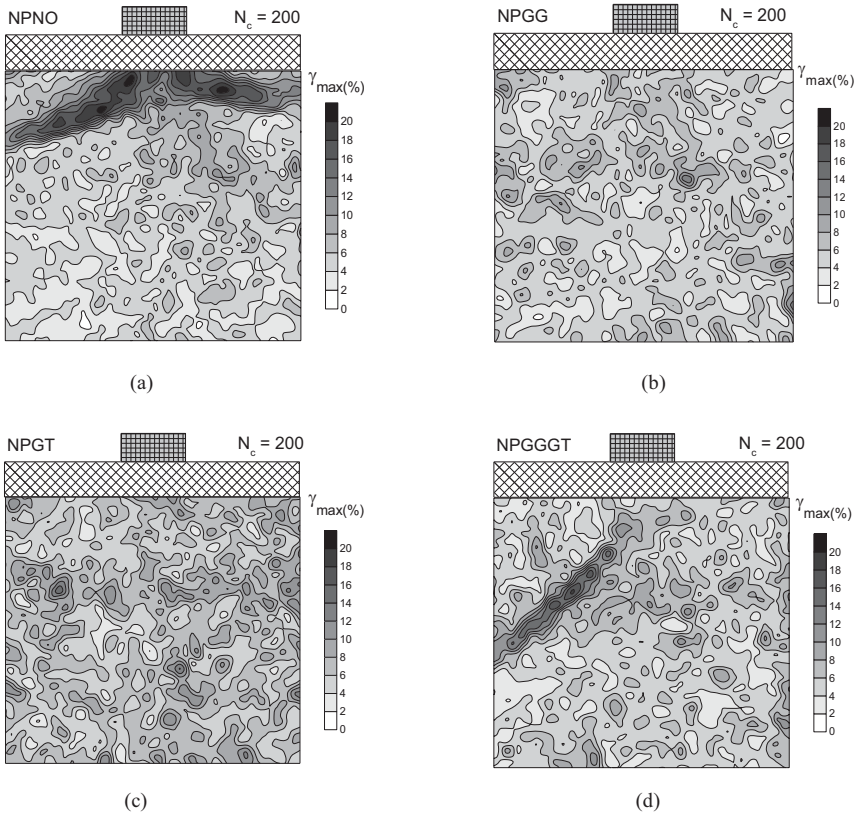

Fig. 9 Maximum shear strain distribution at N_c = 200: (a) NPNO; (b) NPGG; (c) NPGT; and (d) NPGGGT

Figure 8 shows the settlements underneath pavement for all the tested configurations at different selected N_c. They were determined from the vertical nodal displacements of the uppermost-row makers printed on the latex rubber sheet by means of photogrammetric analysis (Figure 1). From Figure 8, the settlement underneath pavements also significantly decreased by reinforcing with geosynthetic reinforcements. Their sequence for NPNO, NPGGGT, NPGG and NPGGGT was the same as the one of footing settlement. From the above, it was realised that reinforcing PMA pavement with geosynthetic reinforcements could improve the rigidity of pavement. Thus, rutting, a distress mechanism in pavement, was probably decreased when reinforcing PMA pavement with geosynthetic reinforcements.

Strain Field of Sand Subbase

Figures 9a, b, c, d show the maximum shear strain (γ_{max}) distribution at N_c = 200 for all the tests performed in this study. It is clearly seen that, for NPNO, the γ_{max} had been already localised to form shear bands spanning from the centre down toward the sides. On the other hand, for NPGG and NPGT, the γ_{max} was fairly uniformly distributed within the area observed while shear band (if any) was unlikely to develop. Nonetheless, for NPGGGT, a shear band spanning from the centre down toward the left was observed. These observations confirms that reinforcing PMA pavement with geosynthetic reinforcements could increase the pavement rigidity such that the vertical stress acting on a small area by the footing was able to widely distributed to the sand underneath. And, when the load was distributed to a larger area, the mobilised shear stress and also the potential of formation for shear band(s) which may lead to failure became small.

Fabric Effective Factor

In this study, fabric effectiveness factor (FEF) was defined as shown in Eq. 1 (Koerner 2005). Its values could be used to quantitatively reflect the effects of reinforcing PMA pavement with different geosynthetic reinforcements. In addition, it may be used in the pavement design either by reducing the design traffic number as shown in Eq. 2 (Koerner 2005) or reducing the pavement thickness. Most importantly, it was a simple index to compare the different performances from the different geosynthetics used.

$$FEF = \frac{\delta_n}{\delta_r} \quad (1)$$

where: δ_n and δ_r are footing settlements at N_c = 200 for unreinforced pavement (NPNO) and pavements reinforced with different geosynthetic reinforcements (NPGG, NPGT and NPGGGT), respectively.

$$DTN_R = \frac{DTN_N}{FEF} \quad (2)$$

where: DTN_R and DTN_N are design traffic number in reinforced and unreinforced pavement, respectively

Table 3 listed the FEF values thus obtained. It may be seen that the value for NPGT (i.e., 2.79) was the highest, about the twice of the second highest for NPGG (i.e., 1.38). On the other hand, the value for NPGGGT was very low (i.e., 1.15), only slightly greater than that of NPNO (1.0). This implied that using the geocomposite for reinforcing of pavement had the highest effectiveness in reduction of the pavement settlement. The difference in the FEF values between NPGT and NPGG was likely due to the fact that geocomposite had a covering ratio of 100 % which is much greater than 25 % for geogrid. And, when the geosynthetic reinforcement was integrated with pavement only by one side by adhering the bottom surface, unlike sandwiched in the pavement material, the less covering ratio could result in less contact area for transferring the stress from the footing to mobilise the tensile force in the geosynthetic reinforcement. On the other hand, for NPGGGT, there are 3 interfaces as shown in Fig. 10. it seemed that the slip plane may occur in second interface (between geocomposite and geogrid), resulted in a very poor performance.

CONCLUSIONS

The following conclusions may be derived:

1. The pavement settlement and maximum shear strain (γ_{max}) distribution in sand underneath decreased by reinforcing PMA pavement with geosynthetic reinforcements.
2. Installation of geosynthetic reinforcement at the pavement bottom could increase the pavement rigidity and distribute the concentrated stress acting on the pavement surface to a much wider area inside the material underneath. This led to distribution of maximum shear strain in a rather uniform manner while the maximum shear strain localisation became unlikely.
3. Under otherwise almost the same physical properties, the pavement settlement when reinforced with geocomposite having a covering ratio of 100 % was much lower than when reinforced with geogrid having much less covering ratio. This was due likely to better integration of geocomposite with the pavement.

Table 3 Fabric effectiveness factor (FEF) determined in this study for quantitatively determination of reinforcing effect

Types of geosynthetic reinforcements	FEF
Geogrid (NPGG)	1.38
Geocomposite (NPGT)	2.79
Geogrid + Geocomposite (NPGGGT)	1.15

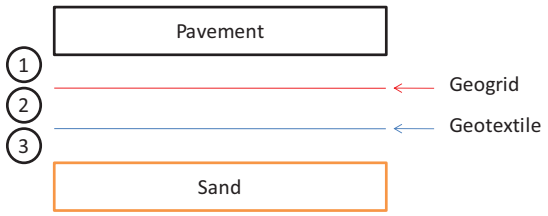

Fig. 10 Schematic of reinforced pavement with geogrid and geocomposite (NPGGGT)

ACKNOWLEDGEMENTS

The polymer modified asphalt cement and geosynthetic reinforcements used in this study were provided by the Tipco Asphalt Public Co., Ltd. and the Polyfelt Geosynthetics Co., Ltd., Thailand, respectively.

REFERENCES

AASHTO (1993). Guide for Design of Pavement Structures, Vol. II. American Association of State Highway and Transportation Officials. Washington, D.C., U.S.A.

Airey G.D. (2004). Styrene butadiene styrene polymer medication of road bitumens. Journal of Materials Science. 99:951–999.

Department of Highways Thailand (1989). Asphalt Concrete or Hot-Mix Asphalt, DH-S 408/2532. Bureau of Materails, Analysis and Inspection.

Department of Highways Thailand (1993). Specification for Polymer Modified Asphalt Cement for Asphalt Concrete (Asphalt Concrete or Hot-mix Asphalt), DH-SP. 408/2536.,Bureau of Materails, Analysis and Inspection.

Glover C.J., Davison R.R., Domke C.H., Ruan Y., Juristyarini P., Knorr D.B. and Jung S.H. (2005). Development of a New Method for Assessing Asphalt Binder Durability with Field Validation, FHWA/TX-03/1872-2, Texas Transportation Institute, College Station, Texas U.S.A.

Koerner R.M. (2005). Designing with Geosynthetics, 5th ed. Pearson Education, Inc. New Jersy.

Kongkitkul W. (2004). Effects of Material Viscous Properties on the Residual Deformation of Geosynthetic-Reinforced Sand. Ph.D. Thesis, The University of Tokyo, Japan.

Kulkarni A.W., Shah M.H, Hai, Decate M.N. and Adhikari A. (1998). Strengthening of overlay against refective and fatique cracking using Proc. Geosynthetic Asia:19-23.

Kunakulsawat V., Punthutaecha K., Youwai S., Kongkitkul W., Jongpradist P. and Maneetes H. (2010). Physical model of reinforced flexible pavement. Proc. 9th International Conference on Geosynthetics. Brazil 3:1551-1554.

Ling H.I. and Liu Z. (2001). Performance of geosynthetic reinforced asphalt pavements. Journal of Geotechical and Geoenvironmental Engineering. ASCE. 127(2):177-184.

Miura S. and Toki S. (1982). A Sample preparation method and its effect on static and cyclic deformation-strength properties of soil. Soils and Foundations. 22(1):.77-61

Sengoz B. and Isikyakar G. (2007). Evaluation of the properties and microstructure of SBS and EVA polymer modified bitumen. Construction and Building Materials. 22:1897–1905.

Thaisri K. (2009). Behavior of Reinforced Flexible Pavement. M. Eng Thesis, King Mongkut's University of Technology Thonburi, Thailand.

Youwai S., Kongkitkul W., Jongpradist P., Anujorn P. and Punthutaecha K. (2010). Geosynthetics in reinforced flexible pavement: Thailand experience, Invited Lecture. Proc. International Symposium, Exhibition, and Short Course on Geotechnical and Geosynthetics Engineering: Challenges and Opportunities on Climate Change, Thailand: 220-233.